Central European Journal of Energetic Materials
ISSN 1733-7178; e-ISSN 2353-1843
Copyright © 2017 Institute of Industrial Organic Chemistry, Poland

Cent. Eur. J. Energ. Mater. 2017, *14*(3): 501-519; DOI: 10.22211/cejem/73825

Nanoaluminium: Is There any Relationship between Particle Size, Non-isothermal Oxidation Data and Ballistics?

Alexander Gromov,[1*] Ulrich Teipel[2]**

[1] *Tomsk Polytechnic University, Lenin Pr. 30, 634050 Tomsk, Russia*
[2] *Nürnberg University of Technology Georg-Simon-Ohm, Wassertorstr. 10, 90489 Nuernberg, Germany*
E-mails: [*]alexander.gromow@th-nuernberg.de, gromov@tpu.ru
[**]ulrich.teipel@th-nuernberg.de

Abstract: This article focuses on data analyses and comparisons for aluminium nanopowders (or nanoaluminium, nAl) reactions under slow (0.5-20.0 K/min, using DTA/DSC/TGA) and fast (>10000 K/min, combustion in solid propellant formulations) non-isothermal oxidation. Particle sizes were defined through the BET method. Active Al content was related with the averaged reactivity parameters, taken from published DTA/DSC/TGA data. The specific oxidation onset temperature for nAl was poorly correlated with the BET particle size under the conditions investigated. Furthermore, the BET particle size exhibited no correlation with the observed ballistic response (burning rate) at 3.0 MPa. A logarithmic correlation $y = 17.484\ \ln(x) - 5813$, with $R^2 = 0.73$, was found between nAl particle size and its aluminium content. A calibration equation for the oxidation onset temperature as a function of nAl particle size was determined as $y = -0.0071x^2 + 3.3173x + 479.32$, with $R^2 = 0.75$. Specific features of the nAl (metallic aluminum content in nAl and the oxidation onset temperature) can be predicted based on the measured powder parameters (such as BET particle size).

Keywords: combustion, thermal analysis, oxidation, nanoaluminium

1 Introduction

Aluminium powders are common ingredients in various energetic systems thanks to metallic aluminium's high combustion enthalpy and availability [1].

In commercial propellant formulations, micron-sized Al powder (or microaluminium, μAl) yields enhanced performance (burning enthalpy, specific impulse and combustion stability) [2, 3]. On the other hand, these advantages are mitigated by aggregation and agglomeration phenomena, resulting in the formation of condensed Al_2O_3 which hinders efficient nozzle expansion of the flow and pollutes the Earth's atmosphere [2, 4-6]. Novel possibilities for the improvement in the performance of energetic systems come from innovative energetic additives such as nanoaluminium [7-13] or so-called 'activated' μAl [14-17]. An investigation of their characteristics is crucial to an understanding of their combustion behaviour and the induced effects on the performance of nanoaluminium-loaded solid propellants.

In the energetic systems community, the term 'nanoaluminium' (nAl) normally relates to ultradispersed (or ultrafine) and very fine powders with an average particle size < 500 nm [18, 19], produced by different techniques [20]. For large scale applications the most promising powder is the electroexplosive nAl (or Alex), with a recent estimated world market of several tons per year [21, 22]. The average electroexplosive nAl has a spherical particle shape and specific surface area of <12 m^2/g, in combination with a metallic aluminium content of 85-95 wt.%. Immediately after production, the nAl powders require passivation or coating procedures to avoid self-ignition and self-sintering of the particles [23-27]. nAl, obtained in inert gas media (argon, nitrogen or their mixtures) by any of the existing methods, is normally pyrophoric in air, because the amount and the rate of heat release from the oxidation reaction is high enough to heat the nanoparticle to its ignition temperature (~670 K for 100 nm nAl particles). The passivation quality defines the chemical stability of nAl and its reactivity in further oxidation processes. The passivation procedure for nAl is not very different from the traditional method of μAl passivation: slow surface oxidation in air or coating with hydrocarbons (industrial μAl with flake particles normally contains 2-3 wt.% of paraffin).

The TEM images reported in [23-25] show the typical structure of air-passivated nAl, with an Al core surrounded by an Al_2O_3 shell. Fresh air-passivated nAl particles are usually characterized by Al_2O_3 shell thicknesses in the range 2 nm to 6 nm, irrespective of particle size. The amorphous oxide layers on nAl particles become crystallized at a defined thickness (7-8 nm) during a storage period of 2-3 years at room temperature [26]. However, none of the existing passivation approaches [27-30] allow nAl particles to reach values of the metallic aluminium content comparable with μAl's metallic content (98-99 wt.%), even assuming large clusters to be present in nAl.

Many of the literature studies have dealt with the reactivity characterization of nAl, while the ageing effects on nano-sized energetic additives have not been

Copyright © 2017 Institute of Industrial Organic Chemistry, Poland

investigated in detail. In spite of this, available data suggest that these powders are highly sensitive to the storage environmental conditions [26, 31, 32].

A better understanding of nAl's energetic performance is still needed, although interest in nAl has been reawakened since the 1990`s [33]. One of the most convenient and common methods for Al particle characterization is the identification of *reactivity parameters* based on non-isothermal oxidation curves (DTA/DSC/TGA) suggested by Il'in *et al.* [34]. While there are comprehensive and detailed experimental data on nAl thermal characterization from different groups in the world [23, 30, 34, 35], the absence of a common, standard procedure for thermal analysis data reduction leads to confusing and misleading interpretation of the results for nAl thermal analysis.

A clarification of the correlation of non-isothermal slow oxidation with the ballistics of nAl-loaded solid propellants would open new avenues in sequestering the amount of burning tests, and thus, have a positive effect on the atmospheric ecological situation in general. In the present work we have made an attempt to correlate these findings and the trend analyses between the most common physical parameters of nAl, its slow oxidation by DTA/DSC/TGA and the fast oxidation by combustion of nAl-loaded solid propellants.

2 Experimental Data on the Non-isothermal Oxidation of nAl

2.1 Particle characteristics of nAl

Particles of μAl with a_s >1 μm contain, on average, more than 98 wt.% of aluminium metal while nAl never exhibits the same properties: usually 2-4 wt.% of powder is occupied by adsorbed and chemisorbed gases, 3-11 wt.% is represented by an aluminium oxide/hydroxide layer on each particle (Figure 1a) and only the residue is the non-oxidized aluminium metal.

The SEM image (Figure 1b) shows nAl clusters of regularly shaped and smooth spheres, with a few non-spherical particles. The clusters are formed due to the extremely high surface tension of nanoparticles yielding particle-particle interactions in a liquid state immediately after wire destruction by explosion in the production process. The multiple necks between the particles are visible in Figure 1b. These necks indicate the common problem of nAl produced by the electrical explosion of wires method: particles might have a very high specific surface area and be severely sintered at the same time. The clusters of nanoparticles can reach micrometric sizes. Cluster formation cannot be avoided by any after-treatment under the passivating/coating procedures due to the necks formed between the particles [23].

Copyright © 2017 Institute of Industrial Organic Chemistry, Poland

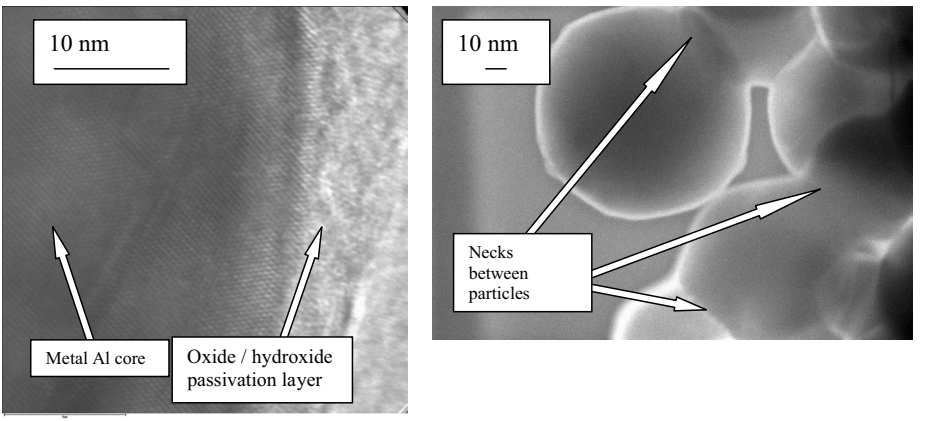

a **b**

Figure 1. Images of air-passivated nAl: (a) individual particle, TEM; (b) cluster of particles, SEM

2.2 Non-isothermal *slow* oxidation of nAl (heating rate 0.5-20.0 K/min)

2.2.1 Reactivity parameters

The non-isothermal oxidation data for this work was extracted from the authors' own publications and from other authors' data obtained under the same experimental conditions. The *reactivity parameters* of non-isothermal oxidation enable comparisons of Al powders with different particle diameters (from 10 nm to the micron-sized range) and surface characteristics (passivation layers, coatings) under various heating rates (from 0.5 K/min to 20.0 K/min) and oxidizing atmospheres (Ar + additives, N_2, Air, O_2).

A broad dataset for slow oxidation (0.5-20.0 K/min) of nAl in N_2/air is given in this work. For the tests performed, the *reactivity parameters* [34] are considered. For Al powder characterization, these can be determined from the DTA/DSC/TGA curves:

1. Oxidation onset temperature, K;
2. Heat released over a temperature range under consideration, J/g;
3. $Al \rightarrow Al_2O_3$ conversion factor, %;
4. Oxidation rate, g/K or g/s.

The reactivity parameters are in fact the most convenient criteria for the relative grading and comparison of Al powders. An overview of the definition of nAl reactivity parameters is given in Figure 2. Typical DTA/DSC traces of air-passivated nAl show an intense oxidation peak before the endotherm

Copyright © 2017 Institute of Industrial Organic Chemistry, Poland

corresponding to Al melting (T = 933 K). Intense Al oxidation before melting is one of the peculiar features of nAl, providing its enhanced reactivity with respect to μAl; due to the lower reactivity of μAl, its intensive oxidation starts above Al melting point (T = 933 K). For μAl powders ASD-4 and ASD-1, with BET particle diameters of 9 μm and 80 μm respectively, the oxidation onset temperatures were 1093 K and 1193 K [36].

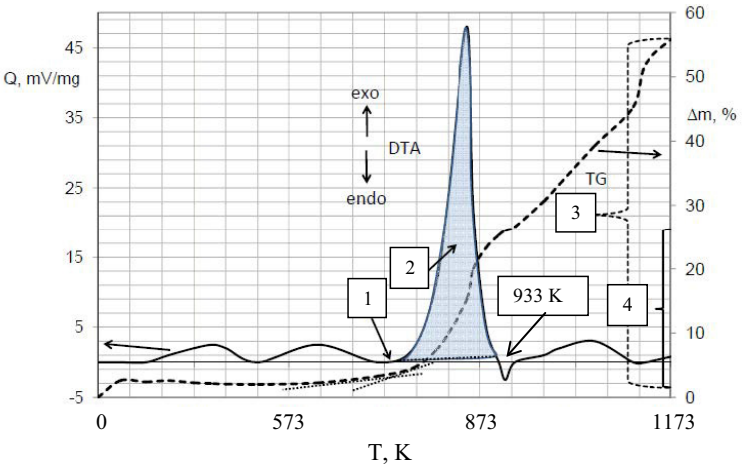

Figure 2. Reactivity parameters taken from DTA/TGA data for a typical nAl powder: 1 − Oxidation onset temperature, K; 2 − Heat released before Al melting, J/g; 3 − Overall powder mass gain over the investigated temperature range, %; 4 − Mass gain before Al melting, %

Two relatively small exothermic peaks before the nAl intense oxidation appeared on the DTA/DSC curves due to adsorbed gas desorption and simultaneous surface oxidation (Figure 2). An exothermic peak after Al melting appeared on the DTA/DSC of nAl due to the oxidation of the largest particles which are always present in the powder obtained.

2.2.2 Experimental data on the nAl slow oxidation

One of the very first studies of DTA/TGA non-isothermal oxidation of nAl (Alex) was performed by Mench *et al*. [8], who investigated the thermal behaviour of nAl by non-isothermal oxidation (DTA/TGA, 5-10 K/min) in different atmospheres (He, N_2, air and O_2). In their study Mench *et al*. did not give the direct particle size distribution or surface characterizations for the powders studied, referring to the data of Ismail and Hawkins [37]. At a heating rate of 5 K/min in air, an initial

Copyright © 2017 Institute of Industrial Organic Chemistry, Poland

intense oxidation onset peak at 803 K was identified [8]. Two other exothermic peaks (973 K and 1303 K) were observed in the DTA traces after the Al melting endotherm (T = 933 K). This behaviour was contrasted with a conventional μAl (20 μm) powder [36]. The latter showed the exothermic reactions at T > 933 K and a deep endotherm corresponding to Al melting. The enhanced reactivity of the nAl powders, with respect to their micron-sized counterparts, was related to their high specific surface area. The authors of [8] explained the chemical processes accompanying nAl reactions with N_2/air in a simplistic manner, because at that time (19 years ago) nAl was a new energetic material with almost unknown properties.

An overview of the Jones *et al*. and Kwok *et al*. experimental results on nAl powders and their effect on energetic systems is reported in [38-41]. The ageing of Alex powder during storage causes the oxidation onset temperature to decrease [41]. This is probably due to the Al_2O_3 shell thickening, reducing the metallic aluminium content inside the particle. Thus, the smaller amount of Al inside the Al_2O_3 shell for an aged particle heated faster and ignited more easily in comparison with the non-aged particle where the amount of Al metal was larger [42]. This experimental phenomenon was also confirmed for μAl particles: aged powders were easily ignited and burnt in air while fresh ones did not [43].

Eisenreich *et al*. [44] investigated the non-isothermal oxidation of several Al powders by TGA (5 K/min, air). The powders tested ranged from Alex (mean-surface particle diameter a_s = 100-150 nm) to μAl (9 μm). In the range 650 K < T < 950 K, only two powders, Alex and sub-micrometric Al with a nominal particle size in the particle diameter range from 300 nm to 700 nm, exhibited a mass increase of more than 10% before the Al melting point. Thus, the intensive oxidation before Al melting is a process characteristic only for nAl and its analogues. Sossi *et al*. [30] investigated the non-isothermal oxidation of different nAl powders, including Alex and air-passivated fluorohydrocarbon-coated Alex. Under the tested conditions (air, 10 K/min), the oxidation onset temperature of air-passivated fluorohydrocarbon-coated Alex was delayed by 36 K with respect to the one for air-passivated Alex. Moreover, the TGA curves showed that the applied fluoropolymer coating was decomposed and/or oxidized before the first Al oxidation exotherm. Chen *et al*. [45] tested the air-passivated nAl produced by laser heating evaporation, with a declared particle size of ca. 50 nm. Tests were performed by DTA/TGA (air, from 5 K/min to 90 K/min). The results can be classified into two categories, depending on the heating rate. For heating rates up to 20 K/min, two exothermic reactions (before and after Al melting) can be clearly recognized. For heating rates higher than 30 K/min, a unique exothermic peak is visible on the DTA traces. According

Copyright © 2017 Institute of Industrial Organic Chemistry, Poland

to Chen *et al*., the absence of heat release for T > 933 K is due to the more complete Al oxidation induced by the Al_2O_3 shell rupture before Al melting. Rufino *et al*. [46] investigated the thermal properties and structural changes of nAl during non-isothermal oxidation using DSC/TGA (Ar and air, 2-10 K/min). Phase transitions of the Al_2O_3 shell were identified in this study. The Al_2O_3 crystal transitions followed the sequence identified by Trunov *et al*. [47] for the oxidation of μAl. Trunov *et al*. considered TGA/DTA performed in O_2, with heating rates of 5-40 K/min, and made XRD analyses of the partially oxidized powder samples recovered from specific intermediate temperatures, 635 °C, 926 °C and 1020 °C. Trunov *et al*. [47] proposed the following reactions for Al oxidation: from 300 °C to about 550 °C the thickness of the natural amorphous alumina layer on the particle surface increases. The rate of this process is controlled by the outward diffusion of Al cations. A transformation of the amorphous alumina into γ-Al_2O_3 occurs at about 550 °C, when the oxide layer thickness exceeds the critical thickness of amorphous alumina (~4 nm). The density of γ-Al_2O_3 is greater than that of amorphous alumina, and the newly formed γ-Al_2O_3 nanocrystallites produce a monolayer only partially covering the aluminium surface. A bare aluminium surface is produced as a result of the amorphous γ-Al_2O_3 transformation. The oxidation rate then increases rapidly until the γ-Al_2O_3 coverage becomes multilayered and continuous. The growth of a continuous γ-Al_2O_3 layer and its partial transformation into the structurally similar θ-Al_2O_3 polymorph occurs thereafter. The oxidation ends when the formation of a dense and stable α-Al_2O_3 occurs, resulting in an abrupt decrease in the oxidation rate. On the basis of reference [48], simplified Al_2O_3 polymorphic phase transition during particle oxidation is known (1).

$$\text{amorphous} \rightarrow \gamma \rightarrow \theta \rightarrow \alpha \quad (1)$$

γ-Al_2O_3 exhibits a higher density than the amorphous one, thus during the amorphous → γ transition, the particle surface is partially exposed with increased conversion to γ-Al_2O_3 in the oxidizing environment. This accounts for the nAl stepwise mass increase observed for T < 933 K. However, when the Al melting temperature is reached for small particles like nAl, the reaction surface is sharply decreased due to the liquid phase released from the oxide shell. Moreover, even by T = 900-1000 K, Al starts reacting with Al_2O_3, with volatile suboxides AlO and Al_2O forming according to [49].

Copyright © 2017 Institute of Industrial Organic Chemistry, Poland

2.3 Non-isothermal *fast* oxidation of nAl- loaded in solid propellants by combustion (heating rate > 10000 K/min)

A selection of representative experimental results on the burning rate of nAl-loaded solid propellants (mostly available data), obtained from different groups (Table 1) opened up the possibility to analyze and compare the powder properties, processes of slow non-isothermal oxidation of nAl with its effects on fast non-isothermal oxidation of nAl under solid propellant burning.

Table 1. Enhancement of the burning rate for nAl-loaded solid propellants (presented as the coefficient K) in comparison with μAl-loaded ones (BET particle size 30 μm)

Particle size of nAl [nm]	Powder sample (Production technique, passivation/coating)	Solid propellant formulation (AP /Al /Binder) [wt.%]	K (p = 3.0 MPa)	Ref.
145-154[a]	Alex (electrical explosion of wires)	68/15/17 (HTPB)	1.73-1.76[c]	[5]
363[a]	Al (plasma condensation, coated with hydrocarbon)		1.25[c]	
145-154[a]	Alex (electrical explosion of wires)	68/15/17 (HTPB)	1.77-1.80	[11]
20-80	N.A.	51/15/34 (HTPB)	1.60[b]	[13]
30-100			1.42[b]	
202[a]	Alex (electrical explosion of wires)	68/14/18 (HTPB)	1.52-1.78[d]	[29]
202[a]	Alex (electrical explosion of wires, coated with 1% HTPB)		2.03	
127-136[a]	Alex (electrical explosion of wires)	68/15/17 (HTPB)	1.83-2.08	[58]
363[a]	Al (plasma condensation, coated with hydrocarbon)		1.68	

[a] Evaluated by BET.
[b] Baseline: solid propellant loaded with 34 μm Al spherical particles.
[c] Baseline: solid propellant loaded with 50 μm Al flakes.
[d] Data differing due to the powder dispersion technique.

The very first analysis of nAl use in solid propellants was published by Zeldovich *et al*. in 1975 [50]. Literature data concerning the burning rate

Copyright © 2017 Institute of Industrial Organic Chemistry, Poland

enhancement of nAl-loaded solid propellant formulations, compared to μAl formulations, are presented in Table 1. In the data presented, the effect of nAl on the burning rate was evaluated from the burning rate coefficient K, the ratio of the burning rate for nAl-loaded solid propellant formulations to the burning rate for basic μAl-loaded (30 μm) solid propellant formulations (2).

$$K = r_{b,nAl}/r_{b,Baseline} \quad (2)$$

The parameter K was defined for the pressure p = 3.0 MPa. This pressure was selected as the average among those commonly mentioned in Western and Eastern standards; 1.0 MPa and 4.0 MPa respectively [1, 35]. For particle sizes in the range 20-363 nm, the observed burning rate increase with respect to the baseline was between 25% and 208% for different propellant binders and nAl contents. Visualization of the solid propellant burning surfaces revealed that the nAl produced oxide particles with reduced dimensions [5].

3 Experimental Data Analysis and Discussion

A goal of the thermal characterization of nAl was to compare the reactivity parameters identified by DTA/DSC/TGA and the burning rate of nAl-loaded solid propellants. While there are many factors affecting burning rate enhancement for nAl-loaded solid propellants compared to μAl-loaded ones, we tried to find any possible relationship between the DTA/DSC/TGA reactivity parameters and the burning rate enhancement.

3.1 Analysis of powder characteristics and their comparison with the reactivity parameters of air/moisture passivated nAl

The aim of the statistical treatment for data on nAl available in the literature was to identify a possible correlation between the mean-surface particle diameter obtained *via* BET and metallic aluminium content and the reactivity parameters under non-isothermal oxidation in air.

Powder characteristics can be evaluated according to different analytical methods. This can hinder direct comparison between different datasets. The influence of the data reduction technique on the metallic aluminium content was discussed by Chen *et al*. [45]. Several analytical methods for metallic aluminium determination were used in [45] to provide better accuracy.

In order to analyze a homogeneous dataset for powders tested under similar operating conditions, a statistical process was applied to the selected data

Copyright © 2017 Institute of Industrial Organic Chemistry, Poland

extracted from [23-27, 38-41, and 51-55]. The homogeneous dataset was chosen on the basis of fully characterized powders:

1. Analyzed nAl was produced by electrical explosion of wires (spherical particles) and passivated by air.
2. Mean-surface particle diameter was deduced from the BET method as: $a_s = 6/(\rho_{Al} \cdot S_{sp})$, nm
   where ρ_{Al} is the density of metallic aluminium, kg/m^3; S_{sp} is the specific surface area, m^2/g.
3. Metallic aluminium content within the samples before conducting the oxidation experiments was defined by a volumetric technique [45].
4. Reactivity parameters were used in the reduction of DSC/DTA/TGA data evaluated under the same conditions (heating in air, 10 K/min).

Air-passivated nAl powders were considered, except where otherwise stated. Additional factors, such as non-air-passivated powder studies, made the comparison too chemically complex. Powders whose BET mean-surface particle diameter was in the range 30 nm to 330 nm were grouped and their characteristics were averaged, thus providing a unique database with a given error bar (defined by the coefficient of determination).

The DSC/DTA/TGA data analysis focused on the dependences of the powder characteristics (metallic Al content) and reactivity parameter (temperature of oxidation onset) on the BET mean-surface particle diameter. The data for the analysis, taken from [23-27, 38-41, and 51-55], were generalized and unified when possible. The powder reactivity should be dependent on the particle size distribution too. A specific problem with the definition and comparison of the reactivity parameters is the multimodal size distribution curves for nAl powders [35]. The presence of the fine fraction in nAl (the very left part of the particles size distribution curve) results in a shift of the temperature of oxidation onset to lower temperatures. Intense oxidation (in fact ignition) of the smallest particles results in a significant acceleration of the oxidation in the whole powdery sample. Thus, for nAl, the reaction ability of the powder is dictated by the fraction of finest particles.

The mass of nAl samples increases by 89% in the case of Al_2O_3 formation and by 51% for AlN formation, by the complete theoretical oxidation or nitridation reactions in air or nitrogen. If nAl is oxidized in air at a low heating rate, the final oxidation product is nano α-Al_2O_3 ($T \geq 1273$ K) [8]. The formation of nano γ-Al_2O_3 by slow non-isothermal oxidation (0.5-20.0 K/min) occurs at low temperatures ($T = 673$-773 K) for electroexplosive nAl [23]. Furthermore, the different definitions of the intense oxidation onset temperature and other parameters on the DTA/DSC/TGA curves can lead to confusing comparisons

Copyright © 2017 Institute of Industrial Organic Chemistry, Poland

between different datasets [23-41]. For certain nAl samples with a specific surface area 12 m^2/g, the mass fraction of micron-sized particle clusters (1-3 μm) could be 68 wt.%, but the number of clusters was only 2% of the total number of particles [56].

At low oxidation rates (0.5-20.0 K/min) aluminium was oxidized in air to Al_2O_3 (reaction 3). However at higher oxidation rates on combustion in air, the interaction of aluminium with nitrogen and the subsequent production of AlN should also be taken into account (reaction 4) [42, 43]. Nitride formation by aluminium oxidation in air at low oxidation rates (0.5-20.0 K/min) has never been reported in the literature [42, 43, 57].

$$4\ Al + 3\ O_2 \rightarrow 2\ Al_2O_3, \quad (3)$$

$$Al + ½\ N_2 \rightarrow AlN \quad (4)$$

The defined reactivity parameters were proposed for relative estimation and comparison [34] for different Al powders under non-isothermal oxidation. nAl passivated by organic/inorganic compounds exhibit lower metallic aluminium content (defined total mass of powder, *i.e*. to Al particles plus the additional organic/inorganic compounds) with respect, as a rule, to the air-passivated nAl. nAl passivated by polytetrafluoroethylene and nitrocellulose lowered the oxidation onset temperature with respect to the air-passivated nAl due to the low-temperature (before Al melting) burning of the applied polymers. For example, nitrocellulose decomposed at 200 °C [23].

Data concerning the metallic Al content and mean-surface particle diameter for the investigated nAl powders are reported in Figure 3. The metallic Al content decreased as the particle size was reduced for nAl. This is due to the formation of oxide/hydroxide layers (Al^{3+}) partially consuming the Al^0 content during powder interactions by passivation and storage in the presence of air/moisture. A definite trend can be identified for Al metal content and mean-surface particle diameter over the data presented. A metallic Al content over 90 wt.% is achievable for mean-surface particle diameters over 220 nm. The reduction in metallic Al content with decreasing size is strongly exhibited for mean-surface particle diameters of less than 80 nm. This hinders their application in energetic systems and the interest for them in practice [58, 59]. The trend line for this database can be approximated by a logarithmic curve with a coefficient of determination $R^2 = 0.73$ (Figure 3).

Copyright © 2017 Institute of Industrial Organic Chemistry, Poland

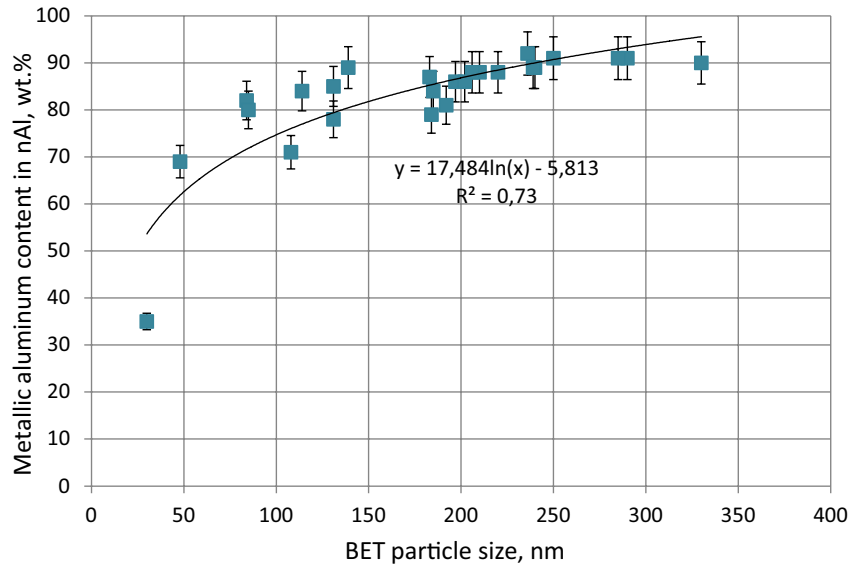

Figure 3. Metallic aluminium content *vs*. mean-surface (BET) particle size for nAl

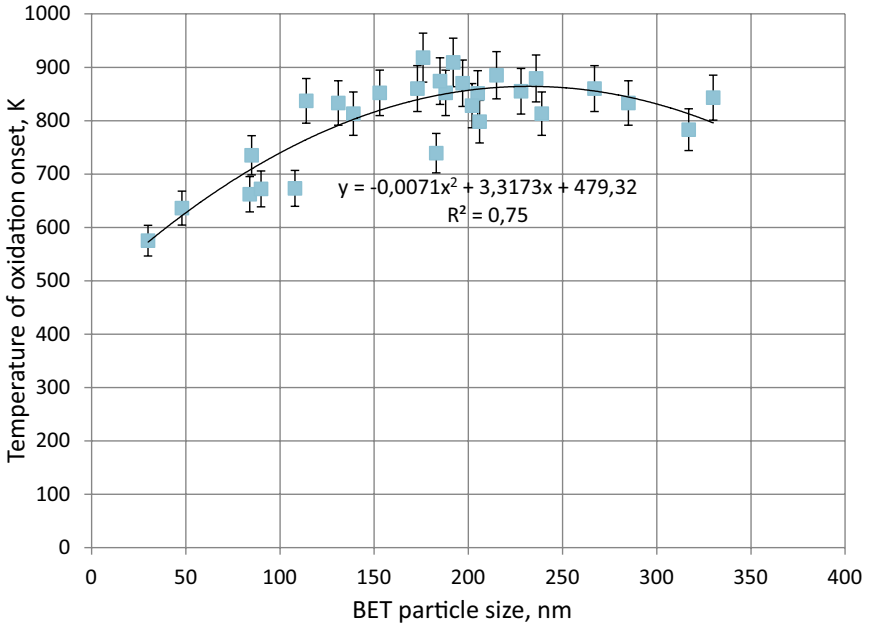

Figure 4. Oxidation onset temperature *vs*. mean-surface (BET) particle size for nAl

Copyright © 2017 Institute of Industrial Organic Chemistry, Poland

Data concerning the oxidation onset temperature is reported in Figure 4. In spite of a relatively high data scatter ($R^2 = 0.75$), the oxidation onset temperature was between 575 K and 920 K for all of the powders tested. Within the selected dataset a correlation can be identified between the BET of the Al powders and their oxidation onset temperatures.

3.2 Nanoaluminium-loaded solid propellants burning

A direct relationship connecting the behaviour of energetic additives (metals) under non-isothermal oxidation (low heating rates, ≤50 K/min) and their effect on the burning of energetic systems (high heating rates, >1000 K/min) have not been identified so far. The analysis performed here is an attempt to identify any possible connections. In order to do this, the homogeneous dataset of the nAl characterized in the non-isothermal oxidation tests and the ones in solid propellant burning experiments was considered.

The dataset presented in Table 1 reports several literature studies of nAl-loaded solid propellant formulations selected from [5, 11, 13, 29, 58]. This choice was made as the selected data on the burning rate also contained values of the BET-based particle sizes, analogous to the data considered for the DSC/DTA/TGA analyses. Thus, the BET values of the particle sizes are present in both cases, for slow and fast oxidation data.

For the evaluation of the effect of nAl on the burning rate, the parameter K (at pressure p = 3.0 MPa) was used (see Table 1). The baseline propellant formulation for evaluation of the burning rate enhancement had the same composition as the nAl-loaded ones, but contained spherical μAl powder (nominal size 30 μm). A possible deviation in the ballistic responses of the nAl-loaded propellant formulations could be due to the poor dispersion of nAl in the solid propellant matrixes and slightly different ingredient details.

The results obtained showed no particular relationship between the nAl behaviour (temperature of oxidation onset) at low heating rates and the ballistic responses (burning rate) of solid propellants loaded with the same material.

4 Conclusions

An effort to find a possible connection between nAl reactivity at low heating rates and burning rate enhancement exhibited by nAl-loaded solid propellants was provided here. The BET based particle size definition and the *reactivity parameter*, onset temperature of oxidation, were considered for the analysis. The analysis focused on the nAl distinctive feature, metal oxidation before the

Copyright © 2017 Institute of Industrial Organic Chemistry, Poland

Al melting (T = 933 K).

These results were considered to investigate a possible relationship between the low heating rate powder oxidation and the burning rate enhancement of nAl-loaded solid propellants. The latter was evaluated by the parameter K (at pressure p = 3.0 MPa).

The results indicated the absence of a possible relationship between the nAl behaviour at low heating rates and its effect on burning rate enhancement. In particular, the high reactivity of nAl yielded intense oxidation onset below T = 933 K that could promote enthalpy release at the burning surface, thus providing an observed enhanced ballistic response.

In general, such a trend in the searched for correlation was not identified, probably because of differences in powder properties [60] and propellant preparation procedures.

However, a logarithmic correlation, $y = 17.484 \ln(x) - 5813$ with $R^2 = 0.73$, between nAl particle size and its aluminium content was found. A calibration equation for the oxidation onset temperature as a function of nAl particle size was determined as $y = -0.0071x^2 + 3.3173x + 479.32$ with $R^2 = 0.75$. The values of the R^2 parameters were rather low, requiring a reassessment when new statistical data appear in the future. On the basis of the trends of the experimental functions found for the analyzed dataset, certain specific features of nAl (metallic aluminum content in nAl and oxidation onset temperature) can be predicted based on measured powder parameters (like BET particle size).

Acknowledgement

The authors thank Professor Luigi DeLuca, Dr. Christian Paravan and the members of SPLab, Politecnico di Milano, for the fruitful discussions and ideas. Financial support of the work was partially provided by the Russian Scientific Foundation (grant 16-19-10316).

Abbreviations and symbols

Alex Aluminium exploded (nAl produced by electrical explosion of wires)
AP Ammonium perchlorate
BET Brunauer-Emmet-Teller theory
DSC Differential scanning calorimetry
DTA Differential thermal analysis
HTPB Hydroxyl terminated polybutadiene
N.A. Not available
TGA Thermogravimetric analysis
XRD X-ray diffraction

Copyright © 2017 Institute of Industrial Organic Chemistry, Poland

nAl Nano-sized aluminium powder, nanoaluminium
μAl Micron-sized aluminium powder, microaluminium
K Burning rate coefficient – ratio of burning rate for nAl-loaded solid propellant formulation to burning rate for basic solid propellant formulation
r_b Burning rate, mm/s
a_s Mean surface (BET) particle diameter, $a_s = 6/(\rho_{Al} \cdot S_{sp})$, nm

References

[1] Kubota, N. *Propellants and Explosives: Thermochemical Aspects of Combustion*. Wiley-VCH, Weinheim, Germany **2002**.
[2] Kuo, K. K.; Summerfield, M. Fundamentals of Solid Propellant Combustion. *AIAA Progress in Aeronautics and Astronautics*. Vol. 90, AIAA, USA, **1984**.
[3] DeLuca, L. T.; Price, E. W.; Summerfield, M. Nonsteady Burning and Combustion Stability of Solid Propellants. *AIAA Progress in Aeronautics and Astronautics*, Vol. 90, AIAA, USA **1992**.
[4] Price, E. W. Combustion of Aluminum in Solid Propellant Flames. *AGARD PEP 53rd Meeting on Solid Rocket Motor Technology*, Paris, France **1979**, Paper 14.
[5] DeLuca, L. T.; Galfetti, L.; Colombo, G.; Maggi, F.; Bandera, A.; Babuk, V. A.; Sindistkii, V. P. Microstructure Effects in Aluminized Solid Rocket Propellants. *J. Propul. Power* **2010**, *26*: 724-732.
[6] Babuk, V. A.; Vasilyev, V. A.; Malakhov, M. S. Condensed Combustion Products at the Burning Surface of Aluminized Solid Propellant. *J. Propul. Power* **1999**, *15*: 783-793.
[7] Ivanov, G. V.; Tepper, F. 'Activated' Aluminum as a Stored Energy Source for Propellants. *Int. J. Energ. Mater. Chem. Propul.* **1997**, *4*: 636-645.
[8] Mench, M. M.; Kuo, K. K.; Yeh, C. L.; Lu, Y. C. Comparison of Thermal Behavior of Regular and Ultra-Fine Aluminum Powders ALEX Made from Plasma Explosion Process. *Combust. Sci. Technol.* **1998**, *135*: 269-292.
[9] Dokhan, A.; Price, E. W.; Sigman, R. K.; Seitzman, J. M. The Effects of Aluminum Particle Size on the Burning Rate and Residual Oxide in Aluminized Propellants. *AIAA* Paper No. 2001-3581, **2001**.
[10] Dokhan, A.; Price, E. W.; Seitzman, J. M.; Sigman, R. K. The Effects of Bimodal Aluminum with Ultrafine Aluminum on the Burning Rates of Solid Propellants. *Proc. Comb. Inst.* **2002**, *29*: 2939-2946.
[11] DeLuca, L. T.; Galfetti, L.; Severini, F.; Meda, L.; Marra, G.; Vorozhtsov, A. B.; Sedoi, V. S; Babuk, V. A. Burning of Nano-Aluminized Composite Rocket Propellants. *Combust., Explos. Shock Waves (Engl. Transl.)* **2005**, *41*: 680-692.
[12] Galfetti, L.; DeLuca, L. T.; Severini, F.; Meda, L.; Marra, G. Pre- and Post-Burning Analysis of Nano-aluminized Solid Rocket Propellants. *Aerosp. Sci. Technol*. **2007**,

Copyright © 2017 Institute of Industrial Organic Chemistry, Poland

11: 26-32.
[13] Jayaraman, K.; Anand, K. V.; Chakravarty, S. R.; Sarathi, R. Effect of Nano-aluminium in Plateau-Burning and Catalyzed Composite Solid Propellant Combustion. *Combust. Flame* **2009**, *156*: 1662-1673.
[14] DeLuca, L. T.; Galfetti, L.; Maggi, F.; Colombo, G.; Reina, A.; Dossi, S.; Consonni, D.; Brambilla, M. Innovative Metallized Formulations for Solid and Hybrid Rocket Propulsion. *Chin. J. Energ. Mater.* **2012**, *20*: 465-474.
[15] Hahma, A. *Method of Improving the Burn-rate and Ignitability of Aluminium Fuel Particles and Aluminium Fuel So Modified*. Patent WO/2004/048,295, **2004**; patentscope.wipo.int/search/en/WO2004048295.
[16] Hahma, A.; Gany, A.; Palovuori, K. Combustion of Activated Aluminum. *Combust. Flame* **2006**, *145*: 464-480.
[17] Maggi, F.; Dossi, S.; Paravan, C.; DeLuca, L. T.; Liljedhal, M. Activated Aluminum Powders for Space Propulsion. *Powder Technology* **2015**, *270*: 46-52.
[18] Morokhov, I. D.; Trusov, L. I. *Ultradispersed Metal Media*. (in Russian) Atomizdat, Moscow **1977**.
[19] Berner, M. K.; Zarko, V. E.; Talawar, M. B. Nanoparticles of Energetic Materials, Synthesis and Properties (Review). *Combust., Explos. Shock Waves (Engl. Transl.)* **2013**, *49*: 625-647.
[20] Storozhenko, P. A.; Guseinov, Sh. L.; Malashin, S. I. Nanodispersed Powders, Synthesis Methods and Practical Applications. *Nanotechnologies* (in Russian) **2009**, *4*: 262-274.
[21] Ivanov, Y. F.; Osmonoliev, M.; Sedoi, V. S.; Arkhipov, V. A.; Bondarchuk, S. S.; Vorozhtsov, A. B.; Korotkikh, A. G.; Kuznetsov, V. T. Productions of Ultra-Fine Powders and Their Use in High Energetic Compositions. *Propellants Explos. Pyrotech.* **2003**, *28*: 319-333.
[22] Sarathi, R.; Sindhu, T. K.; Chakravarty, S. R. Generation of Nano-aluminum Powder Through Wire Explosion Process and its Characterization. *Mater. Charact.* **2007**, *58*: 148-155.
[23] Gromov, A. A.; Ilyin, A. P.; Foerter-Barth, U.; Teipel, U. Effect of the Passivating Coating Type, Particle Size, and Storage Time on Oxidation and Nitridation of Aluminum Powders. *Combust., Explos. Shock Waves (Engl. Transl.)* **2006**, *42*: 177-184.
[24] Gromov, A. A.; Ilyin, A. P.; Förter-Barth, U.; Teipel, U. Characterization of Aluminum Powders, II. Aluminum Nanopowders Passivated by Non-Inert Coatings. *Propellants Explos. Pyrotech.* **2006**, *31*: 401-409.
[25] Kwon, Y. S.; Gromov, A. A.; Ilyin, A. P.; Rim, G. H. Passivation Process for Superfine Aluminum Powders Obtained by Electrical Explosion of Wires. *Appl. Surf. Sci.* **2003**, *211*: 57-67.
[26] Kwon, Y. S.; Gromov, A. A.; Strokova, J. I. Passivation of the Surface of Aluminum Nanopowders by Protective Coatings of the Different Chemical Origin. *Appl. Surf. Sci.* **2007**, *253*: 5558-5564.
[27] Gromov, A.; Strokova, Y.; Ditts, A. Passivation Films on Particles of

Copyright © 2017 Institute of Industrial Organic Chemistry, Poland

Electroexplosion Aluminum Nanopowders, a Review. *Russ*. *J. Chem. Phys. B* **2010**, *4*: 156-169.

[28] Guo, L.; Song, W.; Hu, M.; Xie, C.; Chen, X. Preparation and Reactivity of Aluminum Nanopowders Coated by Hydroxyl-Terminated Polybutadiene HTPB. *Appl. Surf. Sci.* **2008**, *254*: 2413-2417.

[29] Reina, A. *Nano-metal Fuels for Hybrid and Solid Propulsion*. PhD Dissertation, Politecnico di Milano, Department of Aerospace Science and Technology, **2013**.

[30] Sossi, A.; Duranti, E.; Paravan, C.; DeLuca, L. T.; Vorozhtsov, A. B.; Gromov, A. A.; Pautova, Y. I.; Lerner, M. I.; Rodkevich, N. G. Nonisothermal Oxidation of Aluminum Nanopowders Coated by Hydrocarbons and Fluorohydrocarbons. *Appl. Surface Sci.* **2013**, *271*: 337-343.

[31] Cliff, M.; Tepper, F.; Lisetsky, V. Ageing Characteristics of ALEX™ Nanosized Aluminum. *AIAA* Paper 2001-3287, **2001**.

[32] Cerri, S.; Bohn, M. A.; Menke, K.; Galfetti, L. Ageing Behavior of HTPB-based Rocket Propellant Formulations. *Cent. Eur. J. Energ. Mater*. **2006**, *6*: 149-165.

[33] Ivanov, G. V.; Tepper. **F.** 'Activated' Aluminum as a Stored Energy Source for Propellants. (Kuo, K. K. *et al*., Eds.) *Challenges in Propellants and Combustion 100 Years after Nobel*, Begell House, New York **1997**, pp. 636-645.

[34] Il'in, A. P.; Gromov, A. A.; Yablunovskii, G. V. Reactivity of Aluminum Powders. *Combust., Explos. Shock Waves (Engl. Transl.)* **2001**, *37*: 418-422.

[35] *Metal Nanopowders, Production, Characterization, and Energetic Applications*. (Gromov, A.; Teipel, U., Eds.), Wiley VCH, **2014**, p. 430.

[36] Ilyin, A. P.; Gromov, A. A.; An, V.; Faubert, F.; de Izarra, C.; Espagnacq, A.; Brunet, L. Characterization of Aluminum Powders I. Parameters of Reactivity of Aluminum Powders. *Propellants Explos. Pyrotech.* **2002**, *27*: 361-364.

[37] Ismail, I. M. K.; Hawkins, T. W. Evaluation of Electro-exploded Aluminum ALEX for Rocket Propulsion. *CPIA Publication* **1996**, *650* H: 25-39.

[38] Jones, D. E. G.; Brousseau, P.; Fouchard, R. C.; Turcotte, A. M.; Kwok, Q. S. M. Thermal Characterization of Passivated Nanometer Size Aluminium Powders. *J. Therm. Anal. Calorim.* **2000**, *61*: 805-818.

[39] Kwok, Q. S. M.; Fouchard, R. C.; Turcotte, A. M.; Lightfoot, P. D.; Bowes, R.; Jones, D. E. G. Characterization of Aluminum Nanonopowders Compositions. *Propellants Explos. Pyrotech.* **2002**, *27*: 229-240.

[40] Jones, D. E. G.; Turcotte, R.; Fouchard, R. C.; Kwok, Q. S. M; Turcotte, A. M.; Abdel-Qader, Z. Hazard Characterization of Aluminum Nanopowder Compositions. *Propellants Explos. Pyrotech.* **2003**, *28*: 120-131.

[41] Kwok, Q. S. M.; Badeen, C.; Armstrong, K.; Turcotte, R.; Jones, D. E. G; Gertsman, V. Y. Hazard Characterization of Uncoated and Coated Aluminium Nanopowder Compositions. *J. Propul. Power* **2007**, *23*: 659-668.

[42] Malikova, E.; Pautova, J.; Gromov, A.; Monogarov, K.; Larionov, K.; Teipel, U. On the Mechanism of Zirconium Nitride Formation by Zirconium, Zirconia and Yttria Burning in Air. *J. Solid. State Chem.* **2015**, *230*: 199-208.

[43] Popenko, E. M.; Il'in, A. P.; Gromov, A. M.; Kondratyuk, S. K.; Surgin, V. A.;

Copyright © 2017 Institute of Industrial Organic Chemistry, Poland

Gromov, A. A. Combustion of Mixtures of Commercial Aluminum Powders and Ultrafine Aluminum Powders and Aluminum Oxide in Air. *Combust., Explos. Shock Waves (Engl. Transl.)* **2002**, *38*: 157-162.

[44] Eisenreich, N.; Fietzek, H.; Juez-Lorenzo, M.; Kolarik, V.; Koleczko, A.; Weiser, W. On the Mechanism of Low Temperature Oxidation for Aluminum Particles Down to the Nano-Scale. *Propellants Explos. Pyrotech.* **2004**, *29*: 137-145.

[45] Chen, L.; Song, W. L.; Lv, J.; Chen, X.; Xie, C. Research on the Methods to Determine Metallic Aluminum Content in Aluminum Nanoparticles. *Mater. Chem. Phys.* **2010**, *120*: 670-675.

[46] Rufino, B.; Boulc'h, F.; Coulet, M. V.; Lacroix, G.; Denoyel, R. Influence of Particle Size on Thermal Properties of Aluminum Powder. *Acta Mater.* **2007**, *55*: 2815-2827.

[47] Trunov, M. A.; Schoenitz, M.; Zhu, X.; Dreizin, E. L. Effect of Polymorphic Phase Transformations in Al_2O_3 Film on Oxidation Kinetics of Aluminum Powders. *Combust. Flame.* **2005**, *140*: 310-318.

[48] Levin, I.; Brandon, D. Metastable Alumina Polymorphs: Crystal Structures and Transition Sequences. *J. Am. Ceram. Soc*. **1998**, *81*(8): 1995-2012.

[49] Brewer, L.; Searcy, A. W. The Gaseous Species of the Al-Al_2O_3 System. *J. Am. Chem. Soc.* **1951**, *73*: 5308-5314.

[50] Zeldovich, Y. B., Leipunsky, O. I., Librovich, V. B. *Theory of Non-Stationary Combustion of Powders*. Nauka, Moscow **1975**.

[51] Gromov, A. A.; Ilyin, A. P. Properties of Superfine Aluminum Powder Stabilized by Aluminum Diboride. *Combust., Explos. Shock Waves (Engl. Transl.)* **2002**, *38*: 128-139.

[52] Gromov, A. A.; Förter-Barth, U.; Teipel, U. Aluminum Nanopowders Produced by Electrical Explosion of Wires and Passivated by Non-inert Coatings, Characterisation and Reactivity with Air and Water. *Powder Technol.* **2006**, *164*: 111-115.

[53] Gromov, A. A.; Strokova, Y.; Kabardin, A.; Vorozhtsov, A. B.; Teipel, U Experimental Study of the Effect of Metal Nanopowders on the Decomposition of HMX, AP and AN. *Propellants Explos. Pyrotech.* **2009**, *34*: 506-512.

[54] Kwon, Y. S.; Moon, J. S.; Ilyin, A. P.; Gromov, A. A.; Popenko, E. M. Estimation of the Reactivity of Aluminum Superfine Powders for Energetic Applications. *Comb. Sci. Tech.* **2004**, *176*: 277-288.

[55] Kwon, Y. S.; Gromov, A. A.; Ilyin, A. P. Reactivity of Superfine Aluminum Powders Stabilized by Aluminum Diboride. *Combust. Flame* **2002**, *131*: 349-352.

[56] Korshunov, A V. Influence of Dispersion Aluminum Powders on the Regularities of Their Interaction with Nitrogen. *Rus. J. Phys. Chem. A* **2011**, *85*: 1202-1210.

[57] *Nitride Ceramics – Combustion Synthesis, Properties, and Applications*. (Gromov, A.; Chukhlomina, L., Eds.), Wiley VCH, **2014**, p. 360; ISBN 978-3-527-33755-2.

[58] Conti, A. *Steady Burning and Ignition Properties of Aluminized Solid Rocket Propellants*. MSc Thesis. Politecnico di Milano, Dept. of Aerospace Sciences and

Copyright © 2017 Institute of Industrial Organic Chemistry, Poland

Technologies, **2007**.
[59] Sun, J.; Pantoya, M.; Simon, S. L. Dependence of Size and Size Distribution on Reactivity of Aluminum Nanoparticles in Reactions with Oxygen and MoO_3. *Thermochim. Acta* **2006**, *444*: 117-127.
[60] Lyashko, A. P.; Medvinskii, A. A.; Saveliev, G. G.; Iliin, A. P.; Yavorovskii, N. A. Interaction of Super-finely Dispersed Al Powders with Water. *React. Kinet. Catal. Lett.* **1988**, *37*: 139-144.

Copyright © 2017 Institute of Industrial Organic Chemistry, Poland